

## Transport of Water and Gases through EVA Copolymer Films, EVA<sub>70</sub>/PVC, and EVA<sub>70</sub>/PVC/Gluten Blends

S. Marais\*, Q. T. Nguyen, D. Langevin, and M. Métayer

Laboratoire "Polymères, Biopolymères, Membranes", UMR 6522, Université de Rouen / CNRS, UFR des Sciences, 76821 Mont-Saint-Aignan Cedex, France

**SUMMARY:** The transport of water vapor and gases (oxygen or carbon dioxide) through poly(ethylene-co-vinyl acetate) (EVA) films of different VA contents and through EVA<sub>70</sub>/PVC and EVA<sub>70</sub>/PVC/gluten blend films, was analysed by permeation measurements.

In the case of water, a plasticization effect on the material is observed for EVA films with more than 33% wt. of VA content and also for the EVA<sub>70</sub>/PVC blend. For EVA of 19 wt.% VA, there is no plasticization, while for LDPE (low density polyethylene) and EVA of 4.5 wt.% VA, the water diffusion coefficient decreases with increasing the water content. A negative plasticization effect was accounted for by an empirical model and attributed to the formation of water clusters in the non polar polymers. The increase in water sorption extent with the VA content leads to a steady increase in the water permeability in the EVA copolymers while for the EVA<sub>70</sub>/PVC blend, the reduced water permeability is explained by the interaction between chlorinated units and polar groups.

In the case of gas permeation, both for O<sub>2</sub> and CO<sub>2</sub> and whatever the VA content of the copolymer used, the experimental curves are characterized by a constant diffusion coefficient. This result is not surprising as it is generally admitted that, gases sorb into rubbery polymers according to Henry's law. By mixing PVC with the EVA of 70% wt. VA, the diffusion coefficients of CO<sub>2</sub> and O<sub>2</sub> are greatly reduced (6 times).

### 1-Introduction

Fresh fruits and vegetables which are living matters sometimes need to be shipped and stored until their consumption. In order to extend their life time, it is necessary to reduce the rates of biochemical reactions which consume oxygen and produce carbon dioxide, ethylene and water<sup>1)</sup>. There is an opposite relationship between the respiratory intensity and the storage time of the fruit and vegetables. Anaerobic fermentation of bio-components under high water and CO<sub>2</sub> contents often leads to bad taste and smell of fruits and vegetables. A better preservation of this type of food can thus be obtained by decreasing the respiratory intensity and the anaerobic fermentation rate *via* a control of oxygen, CO<sub>2</sub> and water vapor permeabilities. This can be obtained with packaging materials exhibiting high H<sub>2</sub>O/CO<sub>2</sub> and CO<sub>2</sub>/O<sub>2</sub> selectivities.

---

\* Corresponding author, stephane.marais@univ-rouen.fr

To obtain more favorable atmosphere for the preservation of some foodstuffs, micro perforation of hydrophobic films like bioriented polypropylene is currently used. The permeability of all gases is enhanced due to the additional convection flow through the created holes. As the bulk flow through holes is much faster than that through the dense polymer, but is non-selective<sup>1)</sup>, such films are only suitable for certain foodstuffs like cheese, where water vapor and CO<sub>2</sub> buildup must be avoided. In order to adapt the packaging materials to the foodstuffs, one can envisage the use of films whose permeability and selectivity to gases and vapors can be modulated according to the atmosphere required to ensure the best preservation of the foodstuff.

In the present work, we prospect the use of copolymers and blends as selective packaging materials. Changes in copolymer or blend composition make it possible to vary the film permeability and selectivity properties. As ethylene-vinyl acetate (EVA) copolymers with vinyl acetate content varying from 2% to 70%, are commercially available, they are worth being studied as packaging materials.

In this paper, we focused our study on the transport properties of water, and pure CO<sub>2</sub> and O<sub>2</sub> gases through EVA films of different VA contents. A miscible binary blend of EVA with polyvinylchloride, and a heterogeneous ternary blend of this binary blend with gluten, a protein exhibiting high CO<sub>2</sub>/O<sub>2</sub> selectivity, were also studied.

## 2-Theoretical Background

The mathematical treatment of diffusion transport is based on the following assumptions<sup>2,3)</sup>:

The polymer film is homogeneous,

The process is fickian, i.e. not time-dependent,

The interfacial sorption (penetrent/polymer) equilibrium is instantaneous and steady,

The mass transfert occurs in the perpendicular direction to the plane sheet.

### Permeation

The mathematical treatment of diffusion transport is based on the following assumptions<sup>3)</sup>:

1) the polymer film is homogeneous, 2) the process is fickian, 3) the interfacial sorption (penetrent/polymer) equilibrium is instantaneous and steady and 4) the mass transfert occurs in the perpendicular direction to the plane sheet.

Concentration and flux profiles,  $C(x,t)$  and  $J(x,t)$ , are described by Fick's laws and the used boundary conditions are:

$$\begin{aligned}
&\text{for } t = 0, \quad C(x,0) = 0 \quad \forall x \in ]0,L[ \\
&\text{at } x = 0, \quad C(0,t) = C_{eq} \quad \forall t \\
&\text{at } x = L, \quad C(L,t) = 0 \quad \forall t
\end{aligned} \tag{1.}$$

For water ( $H_2O$ ) and oxygen ( $O_2$ ), the measurement principle and procedure were described in a previous paper<sup>4</sup>). When the upstream face of a initially dry film is suddenly into contact with an atmosphere at fixed water or oxygen concentration, while the downstream face is swept with a dry gas at the flow rate ( $f$ ), a permeation flux  $J$  occurs through the film. The initially nil flux increases progressively with time up to a limit  $J_{st}$ , which is the typical steady state flux. The variations with time of the reduced water or oxygen flux  $J/J_{st}$  are obtained by integration of Fick's laws according to our specific boundary conditions.

For carbon dioxide ( $CO_2$ ), the measurement of the transport parameters by the time-lag method is based on the variation of the downstream pressure with time. When the upstream face of an initially dry film is suddenly into contact with an atmosphere at fixed carbon dioxide pressure, while the downstream face is kept at a low pressure (under vacuum,  $10^{-3}$  mbar), the carbon dioxide permeation through the film leads to a pressure build-up which is monitored.

The permeability coefficient is the product of gas flux and film thickness divided by the pressure difference  $\Delta p$  between the two faces of the film (or activities  $\Delta a$ ). From the steady state permeation flux  $J$ , it is possible to determine the permeability coefficient  $P$ :

$$P = \frac{J_{st} L}{\Delta X} \tag{2.}$$

where  $L$  is the thickness of the polymer film,  $J_{st}$  the stationary flux,  $\Delta X = \Delta p$  for  $CO_2$  time-lag permeation tests<sup>5</sup>) and  $\Delta X = \Delta a$  for  $H_2O$  and  $O_2$  permeation tests. In pervaporation, at the upstream interface with pure water,  $\Delta a \approx a_h = 1$ . In permeation,  $a_h = p_h/p_{st}$ , where  $p_h$  and  $p_{st}$  are vapor and saturated vapor pressures, respectively. Usually  $P$  is expressed in barrer ( $cc \text{ STP.cm} / \text{cm}^2 \text{s}^{-1} \text{cmHg}$ ).

On the other hand, for  $CO_2$  time-lag permeation, the stationary flux  $J_{st}$  is obtained from the slope of the steady-state part i.e. when the curve of the amount  $Q = f(t)$  is similar to an asymptotic line which correspond to

$$Q = \frac{DC_{eq}S}{L}(t - t_L) = J_{st}S.(t - t_L) \tag{3.}$$

where  $t_L$ , called time-lag, is the intercept on the time axis of the asymptotic line of the curve  $Q=f(t)$ ;  $S$  the exposed area and  $D$  the diffusion coefficient. Thus, for carbon dioxide, the

permeability coefficient  $P$  can be calculated directly by using eqn. (4) or indirectly knowing that

$$Q = S \int_{t=0}^t J(L, t) dt \quad (4.)$$

One of the main problem in the determination of the values of the different quantities which occur in these equations is linked to the determination of the ad-hoc value (or expression) of the diffusion coefficient  $D$ . If we assume that  $D$  is constant, its value can be calculated from at least two different ways:

i) from the time-lag time-lag  $t_L$  <sup>6)</sup>:

$$D_L = \frac{L^2}{6t_L} \quad (5.)$$

ii) from the time  $t_{0.24}$  corresponding to a value of  $J/J_{st} = 0.24$ , i.e. at the inflexion point I of the transient permeation curve <sup>7)</sup>:

$$D_I = \frac{0.091.L^2}{t_{0.24}} \quad (6.)$$

The calculated value of  $D_L$  usually obtained from the curve  $Q = f(t)$  can be also determined on the transient permeation curve at the J point corresponding to a value of  $J/J_{st} = 0.6167$ , for which  $t = t_L$ .

If  $D_L$  is practically found equal to  $D_I$ , the assumption  $D = \text{constant}$  can be generally done. In permeation, the particular case of  $D$  constant is characterized by the reduced curve  $j = f(\tau)$  ( $j = J/J_{st}$ ) and/or  $q = f(\tau)$  ( $q = Q/SLC_{eq}$ ) with  $\tau = Dt/L^2$

$$q = \tau - \frac{1}{6} - \frac{2}{\pi^2} \sum_{n=1}^{\infty} \frac{(-1)^n}{n^2} e^{(-n^2\pi^2\tau)} \quad (7.)$$

$$j = 1 + 2 \sum_{n=1}^{\infty} (-1)^n e^{(-n^2\pi^2\tau)} \quad (8.)$$

This reduced curve  $j = f(\tau)$  shows an inflexion point I ( $\tau_I = 0.091$ ,  $j_I = 0.24$ ), see figure 1a. At this inflexion point I of the plot of the dimensionless flux  $J/J_{st}$  versus the reduced time  $\tau = Dt/L^2$ , the slope  $\alpha$  ( $= \Delta j / \Delta \tau$ ) depends on the  $D$  variation law. When  $D$  is constant, increases, or decreases with concentration,  $\alpha = \alpha_0 = 5.82$ ,  $\alpha > \alpha_0$  or  $\alpha < \alpha_0$ . The slope  $\alpha$  could be used as a significant parameter of the concentration dependence.

If  $D_L$  is different from  $D_I$ , a model which takes into account a possible variation of  $D$  with the concentration  $C$  of sorbed molecules must be tested. The interpretation of the

experimental curves is then more complex and requires the numerical integration of the experimental data. Assuming that the diffusion coefficient generally increases exponentially with the local permeant concentration in the film during the course of water penetration<sup>8,9)</sup> an empirical equation is then used and represents the diffusion plasticization effect of water on the materials<sup>8,9)</sup>:

$$D = D_0 e^{\gamma C} \quad (9.)$$

Where  $D_0$  is the limit diffusion coefficient,  $\gamma$  is the plasticization coefficient and  $C$  the local permeant concentration. To determine the two parameters of this diffusion law, we may use a new method which is described in more details in a separate paper<sup>10)</sup>. During the fitting procedure of the experimental transient flux data, the values of  $D_M (=D_0 e^{\gamma C_{eq}})$ ,  $D_0$ ,  $\gamma$ ,  $C_{eq}$  and  $\bar{D}$  are computed.  $C_{eq}$  is the penetrant concentration in the polymer at sorption equilibrium and  $\bar{D}$  is an integral mean diffusion coefficient which can be used to characterize the average diffusion coefficient of water in the materials.

Now, on the basis of a constant diffusion coefficient, the solubility coefficient  $S$  can be deduced from the general relation<sup>11)</sup>

$$P = DS \quad (10.)$$

Finally, the fundamental parameters characterizing membrane separation performance are the permeability coefficient,  $P$ , and the ideal selectivity,  $\alpha_{A/B}$ . Ideal gas selectivity is the ratio of permeability coefficients of two gases<sup>12)</sup>:

$$\alpha_{A/B} = \frac{P_A}{P_B} = \frac{D_A S_A}{D_B S_B} \quad (11.)$$

where  $P_A$  is the permeability of the more permeable gas and  $P_B$  is the permeability of the less permeable gas in the binary mixture.

### 3-Experimental

#### 3.1-Preparation of membranes

Poly(ethylene-co-vinylacetate) films (EVA) of low vinyl acetate (VA) contents (up to 19 wt. % ) were kindly provided by 3M Corp (Health Care Specialities, 3M Center St Paul, USA). For the sake of simplicity, the weight per cent of vinylacetate is indicated as a subscript of the copolymer name: EVA<sub>70</sub> stands for the copolymer of 70 wt. % VA content.

Poly(ethylene-co-vinylacetate) of high vinyl acetate contents, which are not available under the form of films, were prepared by casting a solution of the appropriate sample (Baymod

type, kindly provided by Bayer Corp. Paris, France) in dichloromethane (10% w/w  $\text{CH}_2\text{Cl}_2$ , at 30°C with agitation for 10 hours) on a glass plate. After solvent evaporation (under vacuum at 25°C), the film was transferred onto a polypropylene nonwoven fabric and was used with its fabric support in the permeation experiments.

The films used in the present study have different thicknesses, ranging from ca. 100 to 250  $\mu\text{m}$ . Corrections were applied to the data in order to make the comparison of the film transport properties possible, assuming eqn. (2) valid for these films.

In this work, to complete our analysis, a low density polyethylene film (PEld) provided by Goodfellow was used as a reference with 0 % VA compared with EVA films.

For the blend of Polyvinylchloride (PVC from Aldrich Chemical Compagny,  $M_n=55000$ ) with EVA of 70 wt. % vinyl acetate content, a solution of 10 wt. % of PVC and EVA (50/50 w/w) in tetrahydrofuran was cast into films, on a glass plate. After solvent evaporation at room temperature, the films were stored in a dessiccator over phosphorus pentoxide until their use. A solution of 10 wt. % of a heterogeneous ternary blend of this binary blend with gluten, a protein exhibiting high  $\text{CO}_2/\text{O}_2$  selectivity, was also prepared (PVC/EVA/Gluten: 40/40/20 w/w/w).

### 3.2-Methods

#### 3.2.1- Permeation methods

##### a) For water and oxygen: gas sweeping technique

The permeameter consists of a measurement cell, a dry nitrogen supply, a hygrometric unit consisting of two sensors and an oxymeter analyzer. The first sensor, a capacitance type hygrometer (gold-plated alumina device, from Shaw Ltd., Bradford, England), was selected because of its fast-response (response time shorter than 3 s), and the second one (chilled mirror hygrometer, General Eastern Instruments, Massachussetts, USA) was used for its high accuracy ( $\pm 0.07$  part per million (volume) of water vapor in a gas). The oxymeter ("Quartz 650L", Cosma, Igny, France) is equipped with an electrochemical gauge which allows the measurement of oxygen concentration from oxygen partial pressures on both sides of a zirconium oxyde partition. This system give the oxygen concentration in ppmV with a response time shorter than 5 s. The precision is  $\pm 1\%$  of the full scale (10 ppm, 100 ppm, 1000 ppm, 1%, 10%, et 100%) and the reliability  $\pm 0,5\%$ .

The previously dried film was placed in the cell and dry nitrogen was flushed in both compartments many hours until a dew point lower than -70°C was obtained. Next, a stream of pure oxygen or liquid water was pumped through the upstream compartment, then the oxygen

or water concentration in the initially dry sweeping gas was monitored in the downstream compartment via the oxymeter and hygrometers and a data acquisition system.

The flux  $J(L,t)$  at the dry interface is obtained from:

$$J(L,t) = \frac{f}{S} 10^{-6} \frac{x^{\text{out}} - x^{\text{in}}}{R T_r} p_i \quad (12.)$$

with  $S$  the film surface area ( $30 \text{ cm}^2$ ),  $R$ , the ideal gas constant, and  $T_r$ , the temperature (in K) of the experiment. The pressures  $x^{\text{in}}$  and  $x^{\text{out}}$  are directly obtained for oxygen or indirectly obtained for water (from  $T_{\text{dp}}$  dew point temperature) of the sweeping gas. In this latter case, concentration  $x$  (ppmV) is calculated from the water vapor pressure  $p$ , which is directly related to the sweeping gas dew points  $T_{\text{dp}}$  at the inlet and the outlet of the cell ( $x \text{ ppmv} = 10^6 p/p_t$ ,  $p_t$  being the total pressure, usually 1 atm.)<sup>5)</sup>.

#### **b) For carbon dioxide (CO<sub>2</sub>): Time-lag technique**

Due to the lack of CO<sub>2</sub> sensor with high enough sensitivity, the time-lag technique was used for CO<sub>2</sub>. The measurement principle of carbon dioxide permeation properties of films is based on the variable pressure method. During all experiments the temperature of permeation apparatus is kept at 25°C. Before measurement, the permeation cell (XX45047 Millipore filtration cell adapted for gas permeation) was completely evacuated by applying vacuum ( $10^{-3}$  mbar) on both sides of the film for at least one hour. Then, the upstream side was provided with the gas under test at pressure  $p_1$  (in our case  $p_1 = 4$  bar). The increase of pressure  $p_2$  in the calibrated downstream volume was measured using a sensitive pressure gauge (0-10 mbar, Effa AW-10-T4) linked to a data acquisition system.

These permeation experiments were carried out on 2 or 3 samples, and about 4 measurements were made per sample. Therefore, the permeation parameters ( $P$ ,  $D_L$  and  $S$ ) were obtained with a precision range from 4 to 10%. The upstream pressure applied to the samples allowed measurements in a reasonable time (a few ten minutes). These pressure conditions were also chosen in such a way that no irreversible modification of the polymer occurs for instance by plasticization effect due to CO<sub>2</sub><sup>13)</sup>.

In this study, all permeation experiments were carried out at 25°C in a thermoregulated chamber.

#### **3.2.2- Fourier Transform Infrared Spectroscopy**

The transmission IR spectra of a low density polyethylene film (LDPE) were obtained with a AVATAR 360 FTIR spectrometer, using ATR (attenuated total reflection), by collecting and

averaging 32 scans, at a resolution of  $2\text{ cm}^{-1}$ . All IR spectra presented in the following are shown in absorbance. For these IR measurements, the same LDPE film was used, before and after heating at  $50^\circ\text{C}$  and under vacuum (in order to remove water molecules).

## 4-Results and Discussion

### 4.1-H<sub>2</sub>O permeability, diffusivity and sorption coefficient

Fig. 1 is a plot of the thickness-corrected fluxes of water permeating through the polymer films when water activity step (from zero to one) is applied on the film's upstream face at time zero of the transient regime as a function of the thickness-corrected time  $t/L^2$ . It is known that in the reduced time scale  $\tau$ , the diffusion coefficient  $D$  is free from the geometry of the film,  $\tau/D = t/L^2$ . This plot takes into account the effect of the film's thickness on the water diffusion and the permeation flux, so that the differences in the permeation patterns represent the intrinsic behavior of the materials. The correction is based on the assumption that the materials are homogeneous, i.e. uniform in properties; this assumption is acceptable insofar as the films were made of dense polymers and were not restricted to any specific orientation. Fig. 1 shows that the steady-state permeation flux and thus the permeability (as the applied driving force is the same in all experiments), increases according to the order: LDPE < EVA<sub>4,5</sub> < EVA<sub>19</sub> < EVA<sub>33</sub> < EVA<sub>50</sub> < EVA<sub>70</sub> < EVA<sub>70</sub>/PVC < EVA<sub>70</sub>/PVC/gluten.

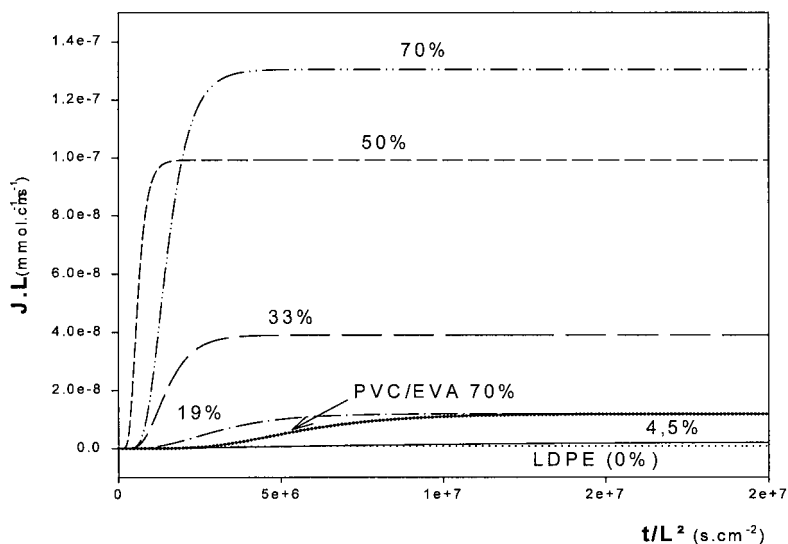


Figure 1. Thickness-corrected fluxes of water permeating through the polymer and blend films.



The water permeability increases steadily with the VA contents (Fig. 1) as one can expect from the increase in the average number of polar groups (carboxyl) in the statistical copolymer.

The transient permeation data were analyzed according to the time-lag method, which is the method generally chosen in the case of gas permeation. For this, the amount of the cumulated permeated water was calculated at each value of time of the transient permeation flux by integration up to this time, then the value of the diffusion coefficient  $D_L$  was determined from the time-lag  $t_L$ . The permeability coefficient was calculated by dividing the thickness-corrected fluxes to the difference in water vapor pressure across the polymer film; this difference is practically equal to the saturation vapor pressure of water at the permeation temperature (2.3756 cm Hg at 25°C<sup>14</sup>), as the water vapor pressure on the permeate side was negligible.

#### **4.2-Dependence of water diffusion coefficient on local water content in polymer films**

The lack of suitable methods for the determination of the diffusion laws when the diffusion coefficient is concentration-dependent generally limits the analysis of the transient permeation regime to the case of constant diffusion coefficient<sup>15</sup>. However, it is easy to show the variation of the diffusion coefficient (with time or with the penetrant concentration in the polymer) when transient permeation data are available: the values of the diffusion coefficient calculated at different extents of the transient permeation, of constant diffusion coefficient, are no longer the same<sup>16</sup>. The values of  $D_I$  and  $D_L$  corresponding to the transient permeation extents of 0.24 and 0.62, respectively, are different for all polymers, except for the EVA of 19 wt. % VA. Tab. 1 shows that the  $D_I$  value is larger than the  $D_L$  value for LDPE and EVA of 4.5wt. % VA, while it is smaller than the  $D_L$  value for the higher % VA. As the former value corresponds to an earlier period of the transient regime compared with the latter one, the smaller  $D_I$  means that the water diffusivity increases as the permeation proceeds from the starting point, where the film is dry. Such an increase in the diffusivity is generally attributed to a plasticization of the materials by the permeant (water), though the origin of the increase in diffusivity with the permeation extent cannot be determined by the transient permeation experiments. We suggest that the decrease in the diffusion coefficient during the permeation process is due to the clustering of water molecules. Indeed, it was reported in the literature that water molecules sorbed in some hydrophobic materials form clusters (to minimize the system free energy), even when the amount of sorbed water is very low<sup>17,18</sup>. To check this assumption, IR measurements were performed with a LDPE film, before and after heating at 50°C under vacuum in order to remove water molecules.

Table 1: Values of the different water diffusion-law parameters obtained for the polar polymers: diffusion coefficient in the dry polymer  $D_0$ , integral mean diffusion coefficient  $\bar{D}$ , plasticization factor  $\gamma C_{eq}$ , plasticization coefficient  $\gamma$ , and the water concentration in the polymer in equilibrium with liquid water  $C_{eq}$ . Concentration-dependent diffusion law used were:  $D = D_0 [\exp(\gamma C)]$  for EVA 19%, to EVA 70%, and the PVC/EVA<sub>70</sub> blend and  $D = D_0 [1 - (\gamma C)^{0.125}]$  for LDPE (0% VA) and EVA 4.5% and  $D = D_0 [1 - (\gamma C)^{0.00175}]$  for the PVC/EVA<sub>70</sub>/Gluten blend, respectively.

EVA % V.A.	L cm.10 <sup>4</sup>	P barrer	D <sub>I</sub> 10 <sup>8</sup> cm <sup>2</sup> s <sup>-1</sup>	D <sub>L</sub> 10 <sup>8</sup> cm <sup>2</sup> s <sup>-1</sup>	D <sub>O</sub> 10 <sup>8</sup> cm <sup>2</sup> s <sup>-1</sup>	$\bar{D}$ 10 <sup>8</sup> cm <sup>2</sup> s <sup>-1</sup>	$\gamma C_{eq}$	$\gamma$ cm <sup>3</sup> /mmol	$C_{eq}$ mmol/cm <sup>3</sup>
O	250	73	9.1	6.7	24.5	12.5	0.76	34.4	0.02
4,5	102	231	1.9	1.5	5.18	2.33	0.80	2.3	0.35
19	102	1134	4.5	4.7	4.5	4.5	0	0	0,26
33	142	3686	8.5	10.1	6.38	14.1	1.42	0,05	27.70
50	243	9357	20.5	25.4	13.3	39.1	1.88	0,07	25.34
70	103	12287	8.1	10	5.09	15.7	1.95	0,02	82.72
35(EVA <sub>70</sub> /PVC)	131	1117	2.25	2.66	1.66	3.65	1.41	4.35	0.32
EVA <sub>70</sub> /PVC/Glu 40/40/20	202	10432	15.9	12.6	12.910 <sup>3</sup>	11.1	4.26	4.26	1.00

The difference between the two spectra of dry and water-saturated LDPE (Fig. 2) suggests that water molecules are under associated form (“clusters”).

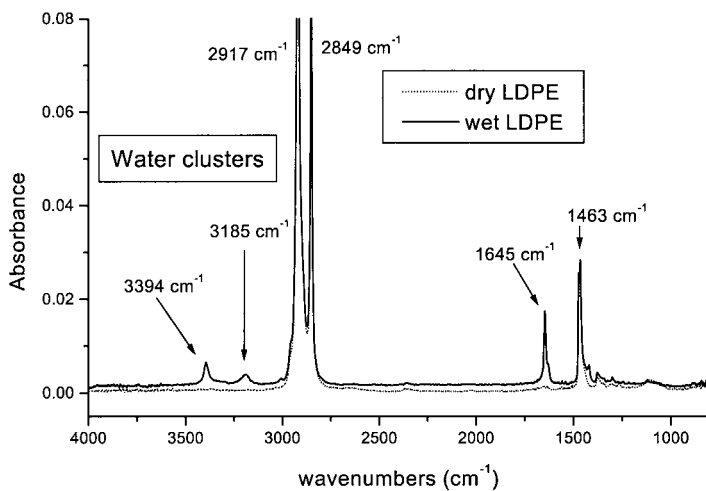


Figure 2. The whole IR spectra obtained on the same LDPE film, wet and dry.

In spite of the very small water quantity, water molecules are not dispersed as individual molecules, but are bonded each other by strong hydrogen bonds as in bulk liquid water. This is clearly shown by the characteristic bands of associated water molecules, at  $3400\text{ cm}^{-1}$  and  $3200\text{ cm}^{-1}$ , respectively for the O-H stretching vibrations, and at  $1645\text{ cm}^{-1}$  for the O-H bending vibrations. The resolution of the large band of the H-bonded associated water molecules into two bands centered at  $3400\text{ cm}^{-1}$  and  $3200\text{ cm}^{-1}$  indicates that bands of the H-bonded water molecules are better defined in the polymer form than those in bulk liquid. It is interesting to note that such a better resolution of H-bonded OH band is similar to that observed for water in a very hydrophilic polymer, poly(vinylalcohol)<sup>19)</sup>. Although such a water molecule clustering in LDPE or EVA 4.5% was not reported before (probably due to the difficulty of experimental determination), we think that clustering is a general phenomenon for water in a hydrophobic medium.

Another way to show the change in the diffusion with the permeation extent is to compare the experimental transient permeation curve with the one calculated with the flux eqn. obtained in the case of a constant diffusivity: the experimental water transient fluxes through the polar polymers are lower than the calculated flux in the early part of the permeation, at times smaller than  $t_l$ , when the polar films are mostly dry. As the permeation proceeds further, more water molecules penetrate into the polar films, plasticize them, leading to larger experimental fluxes compared with the calculated ones (Fig. 3). The reverse situation is observed for the most hydrophobic films (EVA<sub>4.5</sub> and LDPE): the clustering of the water molecules into larger species at high water contents decreases the permeation rate with respect to that predicted from a constant diffusion coefficient<sup>2)</sup> (Fig. 3). When the transient fluxes are computed according to the procedure described in a previous paper<sup>10)</sup>, an excellent agreement between the calculated and the experimental fluxes is obtained with a positive plasticization factor for the polar polymers (Fig. 3), while it was not the case for the hydrophobic films.

The value of the integral mean diffusion coefficient  $\bar{D}$  represents the overall diffusivity of water in the consider polymer; it takes into account the plasticization effect, i.e., the enhancement of water mobility in the polymer due to the presence of sorbed water under given experimental conditions. This means that the increase in the free volume, thus the increase in the diffusivity, due to the added free volume of water, is proportional to VA content in EVA films.

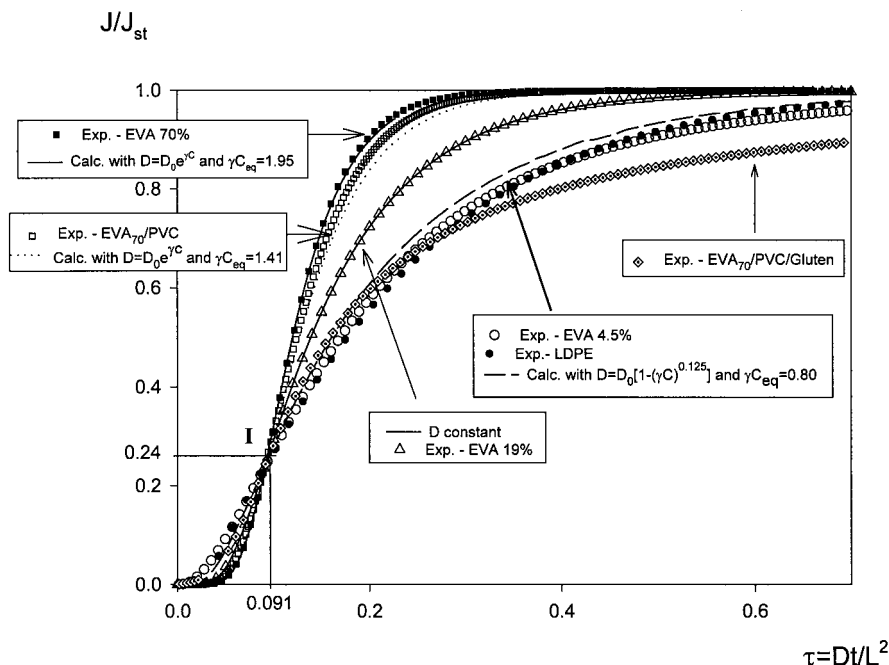


Figure 3. Normalized water transient fluxes through EVA copolymers and EVA<sub>70</sub>/PVC, EVA<sub>70</sub>/PVC/gluten blends.

The EVA<sub>70</sub>/PVC blend shows the smallest water diffusion coefficient (Tab. 1), but the greatest plasticization coefficient. The smallest diffusion coefficient in the dry polymer blend ( $D_0$ ) can be explained either by the largest density of the materials, or the smallest chain segment mobility due to the high PVC density and  $T_g$  compared with those of the EVA component, although this blend is in the rubbery state ( $T_g$  value of the EVA<sub>70</sub>/PVC blend is ca. 10°C). The low segment mobility in this miscible blend can also be caused by the interactions between the two polymer components. Such interactions are shown in Fig. 4 where the shift of the carbonyl vibrations band (from 1734 cm<sup>-1</sup> to 1732 cm<sup>-1</sup>) towards lower wavenumbers indicates the presence of hydrogen bonded C=O in the blend. These should be hydrogen bonds between the hydrogen atoms and the Cl-substituted carbon of PVC with VA carbonyls.

Similar H bonds were already shown for PVC-poly(caprolactones)<sup>20</sup>. However, the fact that the plasticization coefficient is two orders of magnitude larger for the blend with PVC suggests that the chain segment mobility is greatly enhanced by the presence of water molecules.

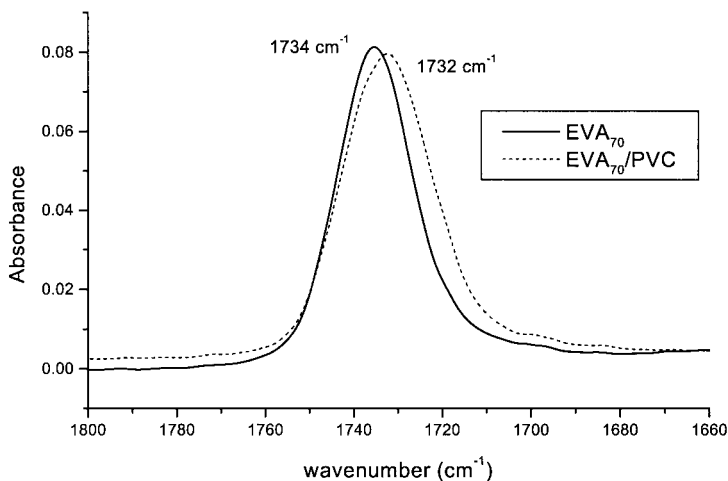


Figure 4. IR spectra of the EVA<sub>70</sub> copolymer and the EVA<sub>70</sub>/PVC blend exhibiting the shift of the carbonyl ( $\text{-C=O-}$ ) band at  $1730\text{ cm}^{-1}$ .

Upon addition of gluten to the PVC/EVA blend, the diffusion coefficient increases significantly (Tab. 1) but is still in the same range as the copolymer of equivalent total EVA content (EVA<sub>33</sub>). As gluten is not miscible to the PVC-EVA phase, such a diffusion coefficient increase cannot be attributed to an enhanced segment mobility of the synthetic polymers. Other possible explanations are i) a high water diffusivity in the gluten phase, and ii) a significant contribution of the water diffusion in the interphase zone close to the gluten particle interfaces. The high water permeability of the blend containing gluten is mainly due to the enhanced water sorption of the disperse gluten phase.

#### 4.3-On the negative plasticization effect

As the exponential law (with a negative plasticization factor) did not lead to a good agreement between the calculated and the observed transient fluxes, we tried to fit the experimental data with different laws in which the diffusion coefficient decreases with increasing permeant concentration. The curve fitting was carried out with a laboratory-made software designed according to the method described in ref. <sup>21)</sup> The best empirical law for the diffusivity dependence on the local water concentration in the polymer (Fig. 3) was obtained for the LDPE, EVA<sub>4.5</sub> and the PVC/EVA<sub>70</sub>/Gluten blend with the following concentration dependence on D:

$$D = D_0[1 - (\gamma C)^n] \quad (13.)$$

For LDPE and EVA<sub>4,5</sub>, the best agreement between the experimental and the calculated data was found for  $n = 0.125$  and for the PVC/EVA<sub>70</sub>/Gluten blend,  $n = 0.0018$ .

This simple law masks a very complex situation. There is a continuous variation of the permeant properties from both the dynamic and statistical viewpoints. As the experiments were carried out at temperature largely above the  $T_g$  value of the dry polymer, the water clustering in polymers should be a relatively slow process, therefore it may influence the overall permeation kinetics. The polyolefins crystallinity may also be modified by the stress created by the formation of large clusters in the matrix. However, considering the very small water concentration at water saturation, this phenomenon must not occur in the present cases. Other parameters which can be affected by the water cluster formation are the system free volume, and the polymer segment mobility. As the LDPE was in the rubbery state in our experiments, the segment mobility is high enough to be affected by small amounts of water. Therefore, the free volume effect would be dominating. However, such free volume data are very difficult to obtain, due to the very low level of water sorption, as that observed for hydrophobic polymers.

The apparent negative plasticization effect would result from the larger size of the aggregated penetrant than that expected from the size of individual penetrant molecules. Additionally, the aggregation of water molecules would further depress the free volume brought about by water, as it is well known that water forms compact globular clusters with pentagonal faces.<sup>22)</sup> However, the penetrant free volume depression alone does not explain the lower water diffusion coefficient in the water- polyolefin system than in the dry polyolefins.

The higher overall water diffusivity in the LDPE can be explained by the higher intrinsic free volume of the LDPE, which is well above its glass transition temperature at the temperature of the measurements. This can be seen in the high value of  $D_0$ , i.e. the water diffusion coefficient in the dry polymers. The  $D_0$  value for the gluten-doped PVC/EVA<sub>70</sub> blend is unusually high. This anomaly may be attributed to the contribution of the fast diffusion loose interphase zone, since  $D_0$  value for the miscible PVC/EVA<sub>70</sub> blend is consistent with the  $D_0$  values for the other films.

The plasticization factor ( $\gamma_C$ ) increases with the VA content in the same way as the permeability (Tab. 1). However, a detailed analysis of the transient fluxes through the EVA films of different VA contents reveals some interesting features. For the sample of 4.5 wt. % VA content, there is a negative plasticization effect in a similar way as in the case of the LDPE homopolymer, but the plasticization coefficient is smaller than that in the homopolymer (Tab. 1). The 19 wt. % VA sample do not experience any plasticization effect on the water diffusion from water molecules. The copolymer samples containing 33, 50, and

70 wt. % VA, respectively, exhibit increasing plasticization factor with the VA content. The increase in the plasticization factor is mainly due to the increase in the water concentration at the polymer face in contact with liquid water (i. e. the water concentration in the materials in equilibrium with liquid water  $C_{eq}$ ).

On the other hand, water seems not to have a strong plasticization effect on the water diffusion in EVA copolymers, even at high VA contents (see  $\gamma$  values in Tab. 1). This behavior can be explained by the relatively high free volume existing in the copolymers (relatively high  $D_0$  values, Tab. 1).

If we admit that the negative plasticization effect is due to aggregation of the water molecules in the hydrophobic environment of the polymer matrix, the fact that this effect vanishes, then is reversed when the content in polar VA groups increases, suggests that the behavior of water in the copolymer is rather governed by an average interaction field than by site interactions. This behavior is consistent with the random nature of the monomer unit distribution in EVA copolymers.

The amount of water sorbed by the blend of EVA with PVC is very low in spite of the polar character of PVC, it is one order of magnitude smaller than that of the pure EVA<sub>33</sub> film of equivalent overall VA content. Again, this behavior can be explained by the interactions between the two polymers which were evidenced by infrared spectroscopy. The interactions between the two polymers reduce the number of polar groups available for interactions with water in the materials.

#### 4.4-CO<sub>2</sub> permeability, diffusivity and sorption coefficient

The sorption coefficient  $S$  increases steadily with VA content in the copolymer (Tab. 2). The blending of the EVA copolymer with the glassy PVC leads to a decrease in the sorption coefficient. Addition of a third glassy component further reduces the sorption coefficient (Tab. 2).

Table 2: Values of CO<sub>2</sub> permeability, diffusivity and solubility coefficients in EVA copolymers/blends of different VA contents obtained at 25°C with the time-lag technique.

EVA % V.A.	L cm.10 <sup>4</sup>	P Barrer	D <sub>L</sub> 10 <sup>8</sup> .cm <sup>2</sup> s <sup>-1</sup>	S cm <sup>3</sup> STP/cm <sup>3</sup> .cmHg
LDPE	250	16	39.6	0.004
19	102	57	45.9	0.01
33	142	30	18	0.02
50	243	70	22.5	0.03
70	103	30	7.8	0.04
35(PVC/EVA <sub>70</sub> )	131	2.26	1.13	0.02
PVC/EVA <sub>70</sub> /Glut	141	6.5	6.7	0.01

It seems that no correlation exists between the time-lag diffusivity and the chemical composition of the materials. In fact, the diffusivity of a gas molecule, for which the sorption coefficient varies moderately with chemical composition, depends on both the segment mobility in the amorphous phase, and the crystallinity of the polymer materials. On the one hand, polar and bulky acetyl groups reduce the chain segment mobility, but on the other hand, the presence of VA units also reduces the crystallinity of the polymer materials, thus enhancing the diffusivity by decreasing the tortuosity of the diffusion path. As gluten is not miscible with the other polymer components, it is only present in the dispersed phase and cannot affect the PVC or EVA segment mobility. The increase in the mean diffusion coefficient upon gluten addition to the PVC/EVA blend also suggests that a fraction of CO<sub>2</sub> passes through low density interphase zones. The small magnitude of the diffusivity increase indicates the absence of interconnected microcracks in the two-phase material. The smallest CO<sub>2</sub> permeability of the PVC/EVA blend is mainly due to the large reduction in CO<sub>2</sub> diffusivity from that of the copolymer. The sorption coefficient increases with the VA contents, in agreement with the data reported by Bondar et al 'for poly(ether-block-amide) copolymers' <sup>23)</sup>.

#### 4.5-O<sub>2</sub> permeability, diffusivity and sorption coefficient

The oxygen permeability, diffusivity and sorption coefficients are in the same range for the tested materials, except for the blend materials (Tab. 3).

Table 3: Values of the permeability, diffusivity and solubility coefficients from the transient permeation data obtained with pure O<sub>2</sub> at 25°C through EVA copolymers/blends of different V.A. contents

EVA % V.A.	L cm.10 <sup>4</sup>	P Barrer	D <sub>I</sub> 10 <sup>8</sup> .cm <sup>2</sup> s <sup>-1</sup>	D <sub>L</sub> 10 <sup>8</sup> .cm <sup>2</sup> s <sup>-1</sup>	S cm <sup>3</sup> STP/cm <sup>3</sup> .cmHg
LDPE	250	2.3	34.1	35.3	0.0007
19	102	5.3	35.1	38.5	0.0014
33	142	10.5	34.5	44.6	0.0023
50	243	8.1	58.0	62.8	0.0013
70	150	3.6	24.5	24.7	0.0040
35(EVA <sub>70</sub> /PVC)	131	0.83	4.27	3.21	0.0026
EVA <sub>70</sub> /PVC/Glut	202	2.19	98.7	94.0	0.0008

The lowest permeability of the PVC/EVA blend is due to its smallest diffusivity. Again, the addition of gluten to this blend enhances the diffusivity but reduces the solubility. Such



changes are similar to those observed for  $\text{CO}_2$  and can thus be interpreted in the same way. It is worth to notice that the  $\text{O}_2$  and  $\text{CO}_2$  sorption coefficients are the same for the  $\text{EVA}_{33}$  sample and the  $\text{PVC/EVA}_{70}$  blend. This suggests that the gas sorption is mainly due to the mean field effect of the VA moieties in the materials.

Except for the polymer blends of PVC, EVA and gluten, the comparison of the normalized experimental flux curves with that calculated for a constant diffusion coefficient (see Fig. 5) shows that oxygen diffusivity through EVA polymer films is rather governed by a constant diffusion coefficient than by a dependence of  $D$  on local penetrant concentration. The same behavior is observed for carbon dioxide. Indeed, all the normalized experimental curves  $Q/\text{SLC}_{\text{eq}}=f(\tau)$  merge together with that calculated for a constant diffusion coefficient (Fig. 6).

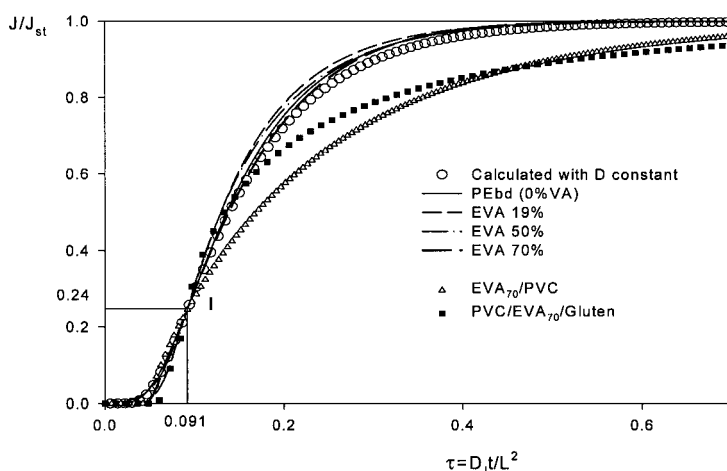


Figure 5. Normalized oxygen transient fluxes through EVA copolymers/blends.

As already reported elsewhere, the sorption coefficient is constant (Henry's law is obeyed) and the diffusion coefficient is independent of concentration<sup>2)</sup> for oxygen and for carbon dioxide at low pressures. As there are no polar interactions between oxygen molecules and with polymer groups, the sorption coefficient for  $\text{O}_2$  is much lower than that for  $\text{CO}_2$ , and varies randomly with the VA content.

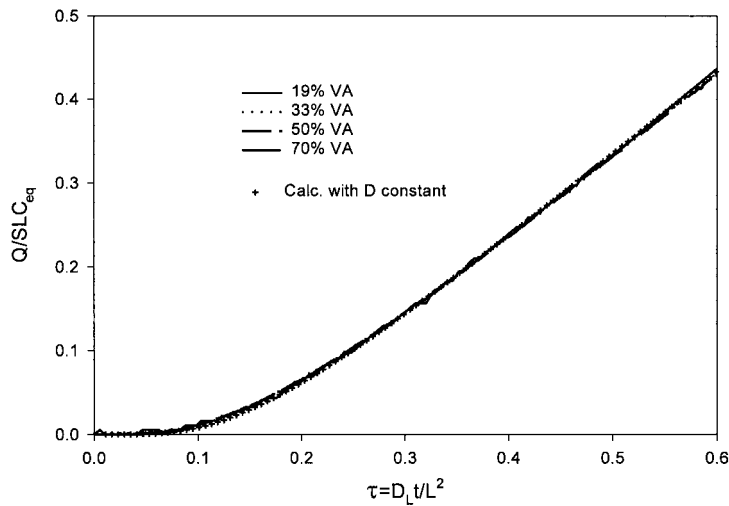


Figure 6. Normalized carbon dioxide cumulated amount through EVA copolymers.

4.6-Ideal selectivities

Tab.4 shows the values of the calculated ideal selectivity for different permeant pairs. The selectivity to water increases with the VA content in the copolymer, and is the highest for the heterogeneous PVC/EVA<sub>70</sub>/gluten blend. The CO<sub>2</sub>/O<sub>2</sub> selectivity is the lowest for the blend of EVA with PVC.

Table 4: Values of the ideal selectivity coefficients from the transient permeation data obtained at 25°C through EVA copolymers/blends of different V.A. contents.

EVA % V.A.	$\alpha_{H_2O/O_2}$	$\alpha_{H_2O/CO_2}$	$\alpha_{CO_2/O_2}$
LDPE	32	4.6	7
19	206	19.9	10.7
33	351	123	2.9
50	1155	134	8.6
70	1445	410	8.3
35(PVC/EVA <sub>70</sub> )	1346	494	2.7
PVC/EVA <sub>70</sub> /Glut.	4763	1605	2.9

From the application viewpoint, PVC/EVA blend is a good candidate for the packaging of bio-products which are sensitive to the water vapor build-up due to biological activities: it limits the respiratory activity *via* its low permeability, and removes efficiently the generated water vapor. With regard to both CO<sub>2</sub> and water selectivity over oxygen, the copolymer film with 70% VA content offers the best performances.

**Acknowledgement:** The authors would like to thank Mrs C. Chappey for the measurements of CO<sub>2</sub>.

## References

1. P. Varoquaux, Films pour la conservation en frais des fruits et légumes, actes de la journée d'études- Séparation des gaz et emballages à perméabilité sélective, Paris/France (1998).
2. J. Crank, G.S. Park, in: Diffusion in polymers. Academic Press, London and New York, 1968.
3. H.S. Carslaw, J.C. Jaeger, in: Conduction of heat in solids. Oxford University Press, second ed. chap. 3 and 12, 1959.
4. M. Métayer, M. Labbé, S. Marais, D. Langevin, M. Brainville, C. Chappey, F. Dreux, P. Belliard. *Polym. Testing*, **18**, 533 (1999).
5. F. P. Glatz, R. Mulhaupt, J. D. Schultze, J. Springer, *J. Membrane Sci.*, **94**, 151(1994).
6. H.L. Frisch. The time Lag in diffusion. *J. Polym. Sci.*, Wash., **61**, 93 (1957).
7. S. Marais, M. Métayer and M. Labbé, *J. Appl. Polym. Sci.*, **74** 3380 (1999).
8. S. Prager, F.A. Long, *J. Am. Chem. Soc.*, **73**, 4072 (1951).
9. S. A. Stern, *J. Membrane Sci.*, **94**, 1 (1994).
10. S. Marais, M. Métayer, Q. T. Nguyen, *Macromol. Theory Simul.*, **9**, 207 (2000).
11. D. W. Van Krevelen, in: Properties of polymers. Their estimation and correlation with chemical structure, Elsevier Scientific publishing compagny, Amstersdam - Oxford - New York, 18 (1976).
12. B. D. Freeman. Basis of permeability/selectivity Tradeoff relations in polymeric gas separation membrane. *Macromol.*, **32**, 375 (1999).
13. M. Wesling, Thesis Enschede, ISBN 90-9005884-2, (1992).
14. Handbook of Chemistry and Physics, 66 th Edition, CRC Press: Boca Raton, 1985; pp D110
15. C. K. Yeom, B. S. Kim, J. M. Lee, *J Membrane Sci.*, **55**, 161 (1999).
16. J. M. Watson, P. A. Payne, *J Membrane Sci.*, **49**, 171 (1990).
17. E. Favre, P. Schaetzel, Q. T. Nguyen, R. Clément, J. Néel, *J Membrane Sci.*, **49**, 171 (1993).
18. S. Marais, M. Metayer, Q. T. Nguyen, M. Labbe, L. Perrin, J.M. Saiter, *Polymer*, **41**, 2667 (2000).
19. F. Huiskens, S. Mohammad-Pooran, O. Werhahn, *Chemical Physics*, **239**, 11 (1998).
20. O. Karal, E. E. Hamurcu, B.M. Baysal, *Polymer*, **38**, 6071 (1997).
21. R. Clément, Q. T. Nguyen, J. M. Grosse, P. Uchytel, *Macromol Theory Simul*, **4**, 921 (1995).
22. H. A. Scheraga, *J Biomol Struct Dynamics*, **16**, 447 (1998).
23. V. I. Bondar, B.D. Freeman, I. Pinnau, Proceedings of the American Chemical Society, Division of polymeric materials, Science Engineering, Las Vegas, **71**, 311 (1997).

